Preprints.org

Spatiotemporal Variability Analysis of Glaciers in the Hindukush Region of Pakistan using Remote Sensing Data

Muhammad Irfan , Muhammad Shafiq [*] , Yasmeen Nergis

Article

Spatiotemporal Variability Analysis of Glaciers in the Hindukush Region of Pakistan using Remote Sensing Data

Muhammad Irfan [1], Muhammad Shafiq [2],* and Yasmeen Nargis [1]

[1] Department of Earth and Environmental Sciences, Bahria University Karachi, Pakistan; irfum3@gmail.com; nergisyasmin.bukc@bahria.edu.pk
[2] Space and Upper Atmosphere Research Commission, SUPARCO, Karachi, Pakistan
* Correspondence: m.shafiq.meteo@gmail.com

Abstract: Headwater in the Indus river in Pakistan is largly dependent on the glaciers located in the northern part of the country alongwith other sources such as direct precipitation. Glaciers are the main source of providing freshwater which provides agriculture and lifeline for millions of people. The hydro-climatological variations in Gilgit watershed of Upper Indus basin are less scientifically understood due to diverse geography, remoteness of the region and larger variations in climatic conditions. These glaciers undergo continuous changes by melting due to global warming or accumulation due to snowfall/precipitation at higher altitudes. In this study, we used remote sensing data to quantify glacier changes in spatiotemporal variability in the past three decades. Five glaciers in the Gilgit region (near the junction of the Hindukush and Karakoram Mountains) with an area of more than 5 square kilometers were selected, namely Phakor, Karamber, East Gammu, Bhort, and Bad-e-Swat glaciers. These glaciers were monitored for changes in their sizes through and cloud free continuous series of Landsat satellite imagery. The annual climatic trends were studied through spatially interpolated gridded climate data WorldClim version-1 climate database for 1970 – 2000. We used it to study the variations of minimum and maximum temperature, solar radiation, and precipitation by preparing sub-sets from the original global grids. The temporal assessment of Bhort, Bad-e-Swat, East Gammu, Karamber, Pokhar glaciers were carried out. It is observed that the glaciers in the Gilgit watershed are rather stable and show no sign of rapid melting or diminishing. The little variability of glaciers extent may be attributed to their geographic condition, altitude, topography, and orientation. The mapped glacier classes have been validated to check the accuracy assessment through an error matrix method. The kappa coefficient from the error matrix has been calculated as 84 % which shows a good agreement. The study makes a critical input towards understanding the dynamics of the glacier in the upper Indus catchment's Gilgit watershed.

Keywords: Indus; Gilgit watershed; hydrological characteristics; glacier changes; Landsat

1. Introduction

Glaciers are considered as one of the most sensitive and reliable indicators for climate change [1]. Generally, the glaciers are taken as continuous source of freshwater contributing into the ecosystem balance and may also lead to hazards such as flashfloods and landslides [2]. Glaciers are generally monitored for hydro-climatological variations, flood risk management, watershed management, and water resource potential. These can be done better through morphometric studies of drainage networks [3]. However, due to their widespread distribution across uneven terrain in a massive region, particularly in rocky places, it is difficult to examine all drainage networks through ground observations or surveys [4]. This constraint has been addressed with the use of radar/optical bsed Digital Elevation Models (DEMs) datasets such as Shuttle Radar Topography Mission (SRTM) and Advanced Space-based Thermal Topography Mission Global Digital Elevation Model (ASTER-GDEM) to be used for delineating drainage systems/ watershed within basins and sub-basins

Pakistan mostly depends on the freshwater supply from the Hindukush-Karakoram-Himalayas (HKH) through the Indus River System running from north to south across the country [5]. For the continuous supply of water, Indus River is mainly feed by the largest glacier cover of the HKH [6]. Climate change has affected the general accumulation and melting of glaciers, which in turn impacts the ecosystem and the economy[7]. Zemp et.al [8] has reported that the overall glacier ice has been reduced globally. Alarmingly, few studies have shown that the HKH glaciers have retreated in past few decades [9], especially the central and eastern glaciers have significantly been reduced in mass [10], hence this literature survey, togather with absence of glacial studies in the Gilgit watershed, provide a good motivation to study the dynamics of the glacier in this study area.

There are many factors contributing to glacier mass loss apart from climate warming; these are atmospheric circulation, cloud cover, rainfall, atmospheric particulate quantities, geo-morphology, and debris layer cover; hence there are differences in the rate of ablation at different places [11,12]. These factors, therefore, pose a great deal of motivation to study the water shortages in South Asia [13]. Gilgit-Baltistan is geographically located in the north of Khyber Pakhtunkhwa province, south of Wakhan Corridor, southwest of China, and comprises an area of 72,971 km². With significant global climatic variations in the last half-century [14], the temperature has increased from 0.32°C to 0.34°C per 10 years as compared with 0.10 °C per 10 years after 1939 [15]. In Gilgit, the hydro-climatological discrepancies of the watershed of the Upper Indus Basin are not as much technically tacit due to various circumstances like inaccessibility of the area, geography, and harsh climatic. Delineation of catchments at numerous scales is made with a strong watershed management skillset. Geographical Information Technology (GIT) and satellite remote sensing (SRS) serve as viable technique to study the watershed.

DEMs have already been used to examine the drainage system in the Gilgit basin region and for the identification of micro-watershed boundaries [16,17]. The pixels based supervised and unsupervised classification methods can be used to delineate the glacier ice and ultimately quantify the glacier area in the region. This study aimed to review and evaluate the seasonal variations of meteorological parameters in the Gilgit Region of Pakistan and temporal variations in glaciel area of Bhort, Bad-e-Swat, East Gammu, Karamber, and Phakor Glaciers during the last three decades through subpixel classification algorithm, indices based supervised classification and object based algorithm using Landsat imageries (multispectral TM, ETM+, and OLI satellite images). The study will generally contribute to the exisiting knowledge of Glaciers behaviours under climate stress as well as specically report the status of HKH glaciers aver the extended period of three decades.

2. Study Area, Datasets and Methodology

Study Area

Gilgit's watershed is a significant source of freshwater in Pakistan's northern area (Figure 1). The HKH region spans approximately 2,000 square kilometers throughout Southeast Asia and borders Afghanistan, Bangladesh, Bhutan, China, India, and Nepal [18]. The watershed is located between 72°25'02" E and 74°19'25" E, and 35°46'05" N and 36°51'16" N. The geographical watershed region is 13,552 square kilometers, with elevations ranging from 1,388 to 6,722 meters [17,19], and is drawn in Figure 2 using elevation data from SRTM at one arc-second resolution. Flash floods, supraglacial lakes, glacier lake outburst floods, and landslides are commonly reported in the region [20–22]

3

Figure 1. The study area.
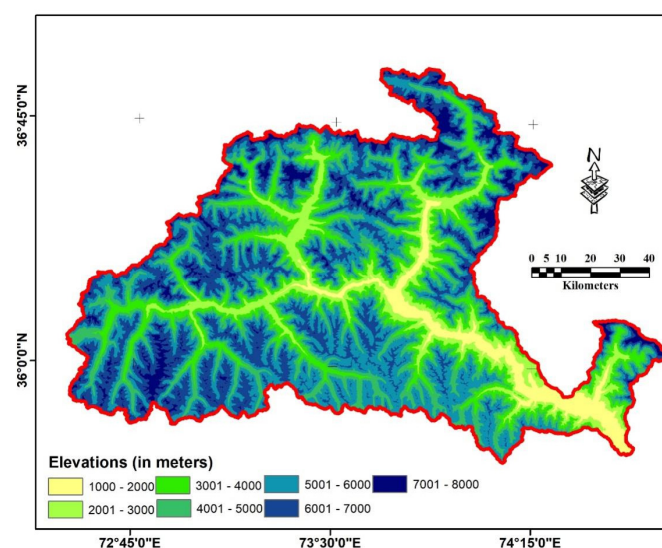
Figure 2. Elevation distribution of study area.

Study of climatological conditions

For numerous uses, records with a high (1 km²) spatial resolution are preferred because they detect ecological deviations that are misplaced at lesser spatial resolutions, especially in hilly and further regions with strong climate inclines. Climate surfaces, or spatially interpolated gridded climate data, are utilized in a variety of applications, primarily in the agricultural, environmental, and biological disciplines. This study uses the climatological data provided by Hijmans et al. (2005) [26] named WorldClim version 1 climate database for 1970-2000, for global land areas, comprising of continuing normal monthly temperature and rainfall [27], being used to study the variations of lowest and extreme temperature, solar energy and precipitation by means of preparation of sub-set from the original global grids.

Glacier Change Analysis

Through multispectral TM, ETM+ and OLI satellite images were used for the study. Each mulyispectral image was subjected to multicriteria segmentation [24], which was futher classified on the basis of shape and spectral pattern [25]. At first, the un-supervised classification techniques were applied, and the results obtained were not so much accurate with visible misclassification of several glacier cover areas. The supervised classification improved the overall accuracy. The glacier mapping using the supervised classification techniques, thus, has been used to delineate the glacier area. To

improve the segmentation accuracy, the spectral pattern was given a higher weighting (70%) than the related shape (30%). The data sets used for glacier change analysis are shown in Table 1.

Table 1. Datasets used in this study.

Satellite / Sensor	Year	Scene ID	Path	Row	Cloud Cover	Acquisition Date
Landsat 5 TM	1988	LT05_L1TP_150035_19881027_20170205_01	150	35	3%	1988-Oct-27
Landsat 5 TM	1994	LT05_L1TP_150035_19940708_20170113_01	150	35	4%	1994-Jul-08
Landsat 7 ETM+	1999	LE07_L1TP_150035_19990916_20170217_01	150	35	1%	1999-Sep-16
Landsat 8 OLI	2014	LC08_L1TP_150035_20140917_20170419_01	150	35	1.25%	2014-Sep-17
Landsat 8 OLI	2018	LC08_L1TP_150035_20180912_20180927_01	150	35	1.41%	2018-Sep-12

Kappa Coefficient

The Kappa coefficient measures of how well the categorization results compare to random values. It can have a range of values from 0 to 1. There is no agreement between the categorized image and the reference image if the kappa coefficient is 0. The categorized picture and the ground truth image are identical if the kappa coefficient is one. As a result, the larger the kappa coefficient, the better the categorization accuracy.

It is calculated from the following relationship.

$$Kappa\ Coefficient\ =\ \frac{Overall\ Accuracy - Random\ Accuracy}{1 - Random\ Accuracy}$$

Through this technique, accuracy was assessed using an error matrix approach and a stratified random sampling method to provide 250 ground truth reference data points. To match the corresponding category, these ground truth locations were overlain on the land use/ land cover map. The generated error matrix and associated category membership resolute by ground truth, placed in the rows and classified cover type determined by this study methodology are placed in columns according to the methodology of Maitima et al.[28]. Correct values lie along the primary diagonal of the matrix when it is arranged in this manner [29]. Classified values are incorrectly placed in the off-diagonal sections of the matrix, making it obvious which class they belong to [30].

3. Results and Discussions

3.1. Temperature profile of Gilgit Watershed

The global grids of monthly averaged 30-year data were obtained, and the study area subset was extracted to obtain the regional temperature values. The interpolated minimum surface temperature processed from the point data from local stations portrays a high value of –0.2°C and a low value of –35.1°C for January. The low-temperature values are mainly observed at higher altitudes on the Northern side and high values of temperature on the lower altitudes on the southeast of Gilgit watershed, respectively. The scale range is 60 km shown in Figure 3. Moreover, January, the severe winter month, has a more projecting T_{min} (low) compared to T_{max} (high). January is the frosty winter coldest month in Gilgit. February, the winter month, has a more projecting Tmin (low) than T_{max} (high). The average high temperature in Gilgit rises slightly from a chilly January to a cool February, the last month of the winter. March is a pleasant month in Gilgit, with temperatures ranging from -13.3°C to 6.8°C on the mean. The mean high temperature in Gilgit climbs in March.

In Gilgit, April is a warm spring month, with average valley temperatures ranging from -7°C to -10°C. The average high temperature climbs in April. May, the penultimate month of spring, is another hot month, with an average valley temperature of 8°C. The average high temperature rises slightly from a moderately hot April to a warm May. June, the first month of summer, is a hot month in Gilgit. July is the hottest month of the year. September is the first month of autumn and is still a hot month. October, like September, is slightly warmer fall month. November is the last month of the

fall and is another weatherly relaxed and cooler month. December is a winter month, with the average min temperature fluctuating at -16°C. Figure 3 shows the spatial distribution of monthly averaged minimum temperature on monthly basis for thirty years.
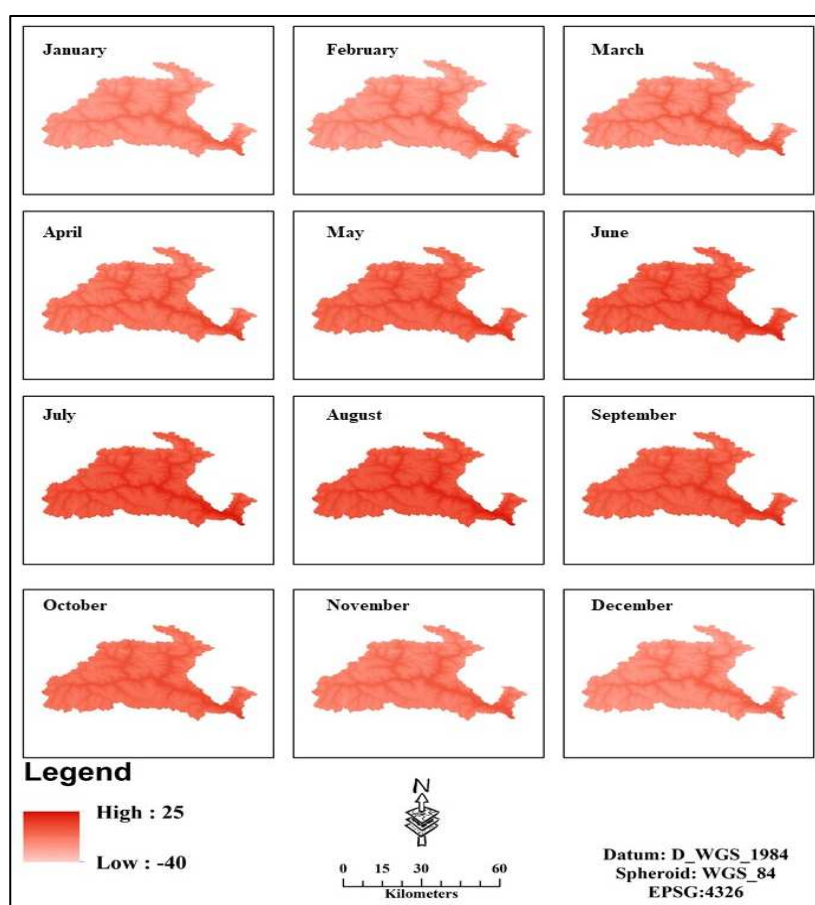
Figure 3. Spatial distribution of monthly averaged minimum temperature (in degrees Celsius) – Normalized matrix of yearly profile.

3.2. Solar Radiation Intensity in the Gilgit Watershed

Radiation from the sun is the principal wellspring of energy for the Earth's temperature framework. Changes in the Earth's circle around the sun cause contrasts in the cyclical circulation and measure of sunlight-based radiation arriving at the earth. Chronicles of past environments show that there is a connection between these multiplicities and long-haul environment changes. Interglacial conditions start with expanding mid-scope summer insolation and end as mid-scope summer insolation diminishes. Normal sunlight in March in Gilgit is 12 hours. The month with the lengthiest days is June (Normal sunlight: 14.6h). The month with the briefest days is December (Average light: 9.8h). Normal daylight in March is 6h while the month with the most daylight is June (Average daylight: 10h). As shown in Figure , the months with the least daylight are January, February, and December, when the typical daylight is 5 hours. The introduced sun-powered radiation information handled from the point information from neighborhood stations, month to month, arrived at the midpoint of 30 years, depicts a high worth of 7545kJ m^{-2} day^{-1} and a low worth of 5641 kJ m^{-2} day^{-1} across watershed for the long stretch of January. The low upsides of sun-powered radiation at the higher heights on the Northern side might be related to the huge measure of overcast cover frequently present at high mountains. Ordinarily, under clear sky conditions, the sun-oriented radiation increments with height. This is known as the height impact. The angle values are ~8% per 1000m of height. Spatial distribution of monthly averaged solar radiation shown in Figure 4.
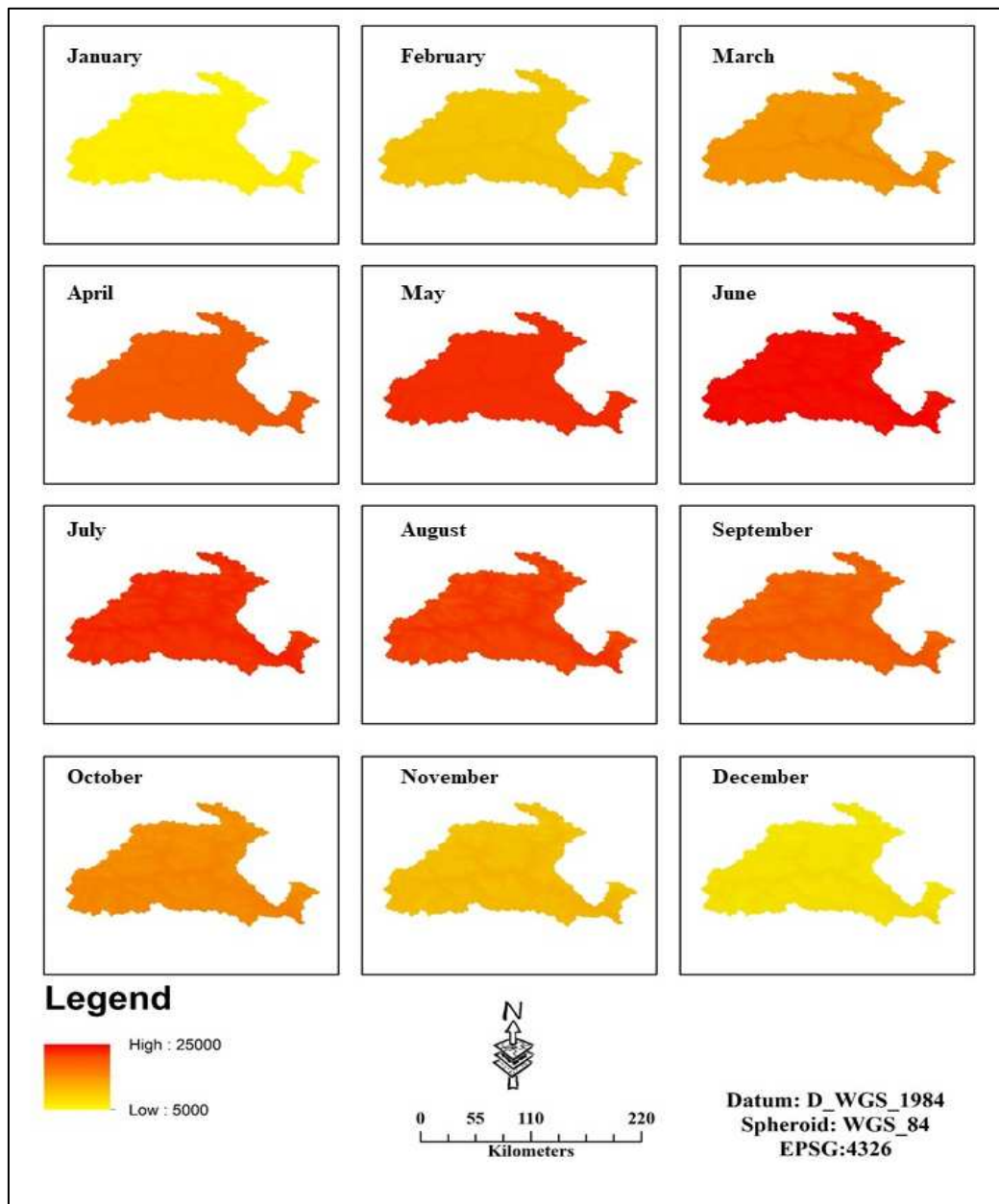
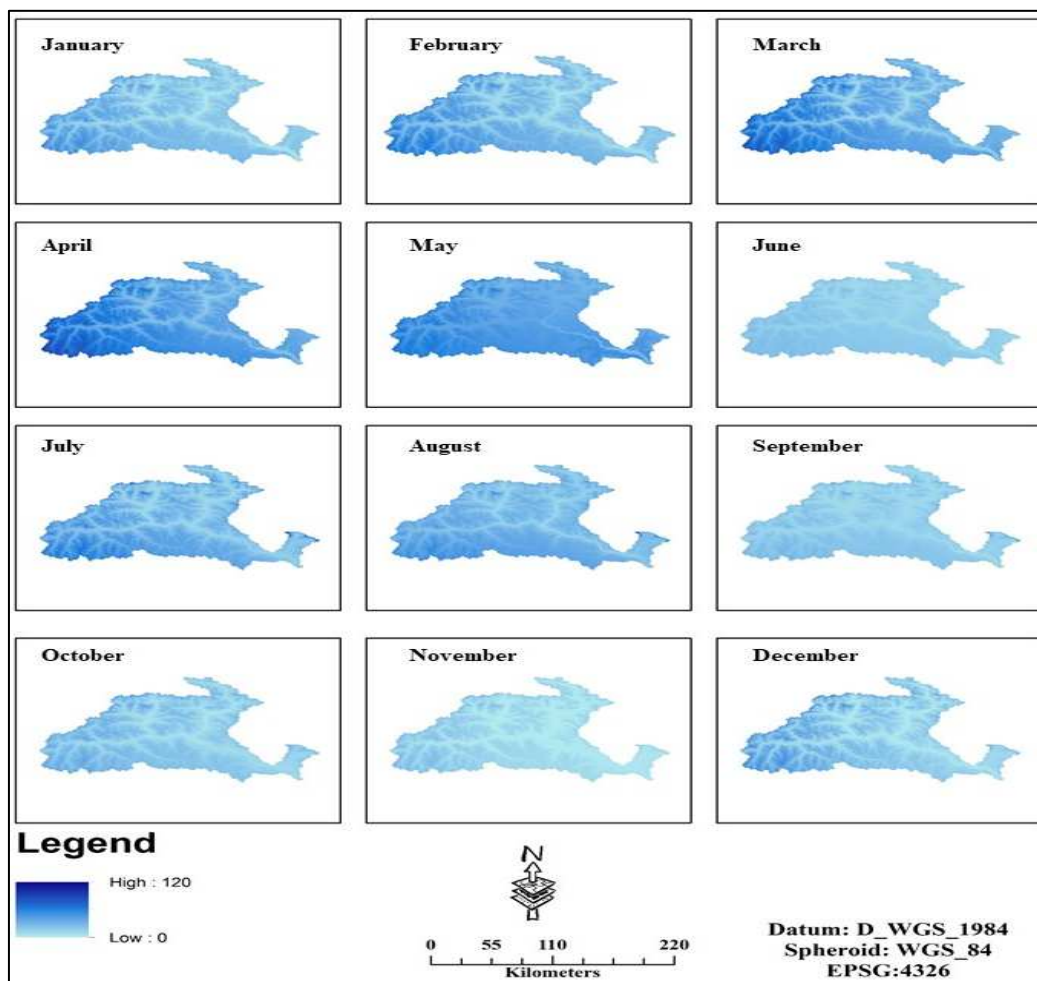**Figure 4.** Spatial distribution of monthly averaged Solar radiation (in kJ m-2 day-1) normalized matrix for yearly profile for Gilgit catchment.

3.3. Precipitation in the Gilgit Watershed

There are four rainy seasons in the study area, viz., wintertime, pre-monsoon, monsoon (rainy and cloud burst season), and post-monsoon precipitation. The town of Gupis is known to have the lowest rainfall in the GB region. Javed et al., (2020) [31] have analyzed the 90-year ground-based point measurements from meteorological observatories operated by the Pak Meteorological Department. However, the study lacks the interpolated analysis at the spatial extent. It is shown that Gupis station gets approx. 13 rainy days in the whole year, excluding the solid precipitation in the form of snow at higher elevations.

The data of observation/measurement of precipitation contain many inaccuracies owing to its spatial and temporal pattern in quantity and intensity. The interpolated precipitation data processed from the point data from local stations, monthly averaged of 30 years, shows values mapped in Figure 5.

Figure 5. Spatial distribution of monthly precipitation (in mm) normalized matrix of yearly profile for Gilgit catchment.

3.4. Glacier Change Analysis

Glacier mapping using the object-based classification techniques has been used to delineate the glacier area. It was observed from the overall results that mostly, glaciers are rather stable, specifically in the Gilgit watershed. The little variability of glaciers is due to their geographic condition, altitude, topography, orientation, and climate conditions. In direction to evaluate the correctness of the glacier mapping, the accuracy assessment was carried out using the error matrix approach with a calculated kappa coefficient value to be 84.14%. The summary of the change detection for the five glaciers of the Gilgit watershed is explained in the coming paragraphs.

3.4.1. Bhort Glacier Change Analysis

The extent coordinates of the Bhort glacier are from 74° 04′ 40″ E to 74° 11′ 10″ E and from 36° 31′ 12″ N to 36° 34′ 04″ N. The elevation of the glacier goes up to 5,784 m and has a max slope of 57%. It was observed that the ice-covered areas have reduced from   14.02 km² in 1988 to 9.91 km² in 2018. However, the debris-covered area was increased from 0.98 km² in 1988 to 2.45 km² in 2018. The overall glacier changes are 15.00, 13.11, 13.00, 12.52, and 11.65 km² for 1988, 1994, 1999, 2014, and 2018, respectively (Figure 6). The results revealed that the overall ice-covered area from 1988 to 2018 has reduced by 4.11 km². However, the overall debris-covered area from 1988 to 2018 has increased by 1.47 sq km.
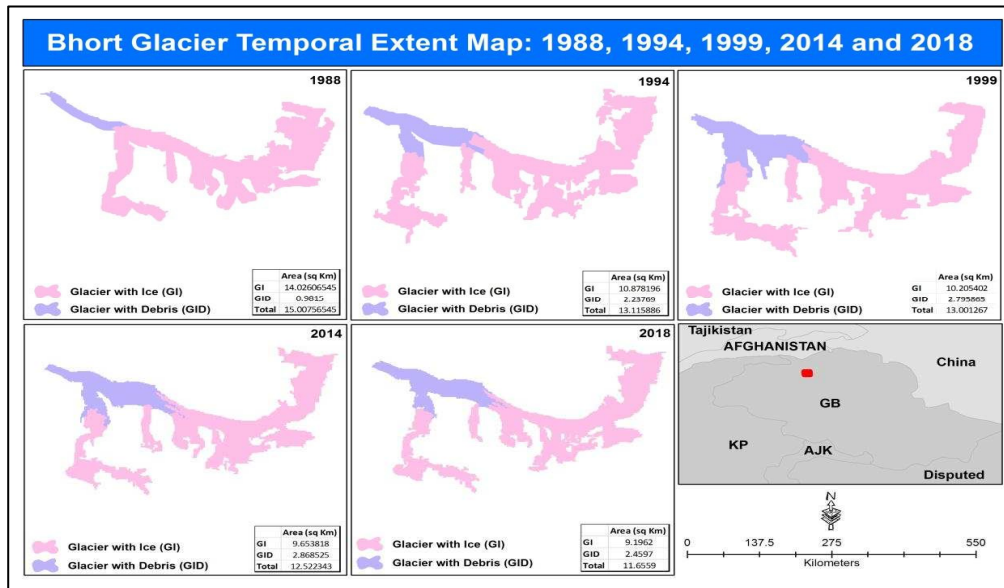
Figure 6. Bhort glacier temporal change extent for the years 1988, 1994, 1999, 2014, and 2018.

3.4.2. Bad-e-Swat Glacier Change Analysis

The extent coordinates of the Bad-e-Swat glacier are from 74° 02' 15'' E to 74°06' 35'' E and from 36°28' 15'' N to 36° 32' 20'' N. The elevation of the glacier goes up to 5,835 m with a max slope of 51%. Figure 7 shows that the overall glacier changes remained 12.24, 14.70, 12.52, 13.78, and 12.67 sq km for 1988, 1994, 1999, 2014, and 2018 respectively. The results revealed that the overall ice-covered area for 30 years has been reduced in all years except 1988, possibly due to climatic changes. However, the debris-covered area from 1988 to 2018 has increased by 0.52 sq km.
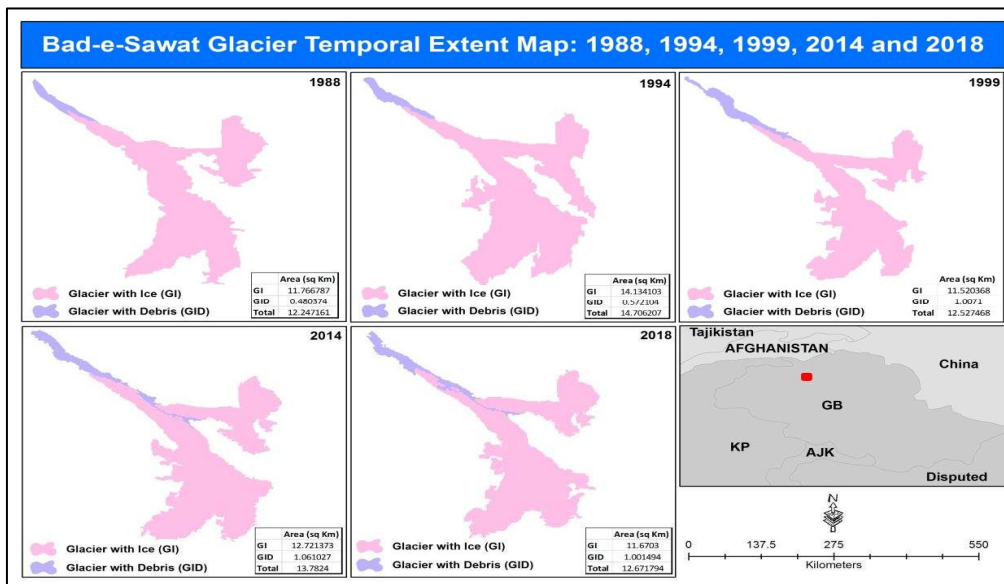

Figure 7. Bad-e-Swat glacier temporal glacier change extent for 1988, 1994, 1999, 2014, and 2018.

3.4.3. East Gammu Glacier

The extent coordinates of the East Gammu glacier are from 73° 19' 30'' E to 73° 24' 10'' E and from 36° 35' 10'' N to 36° 38' 30'' N. The highest elevation of the glacier is 6,379 m with a max slope of 68%. It was observed that the ice-covered areas are 9.02, 12.38, 11.47, 9.97, and 9.77 km^2 for the years 1988, 1994, 1999, 2014, and 2018 respectively. The debris-covered area was 0.68, 0.63, 0.37, 0.47, and 0.32 km^2 for 1988, 1994, 1999, 2014, and 2018 respectively. The overall glacier changes are 9.71,

13.02, 11.84, 10.44, and 10.09 km² for 1988, 1994, 1999, 2014, and 2018 respectively (Figure 8). The debris-covered area from 1988 to 2018 has decreased by 0.37 km² whereas the total ice-covered are has been increased only by 0.75 km².
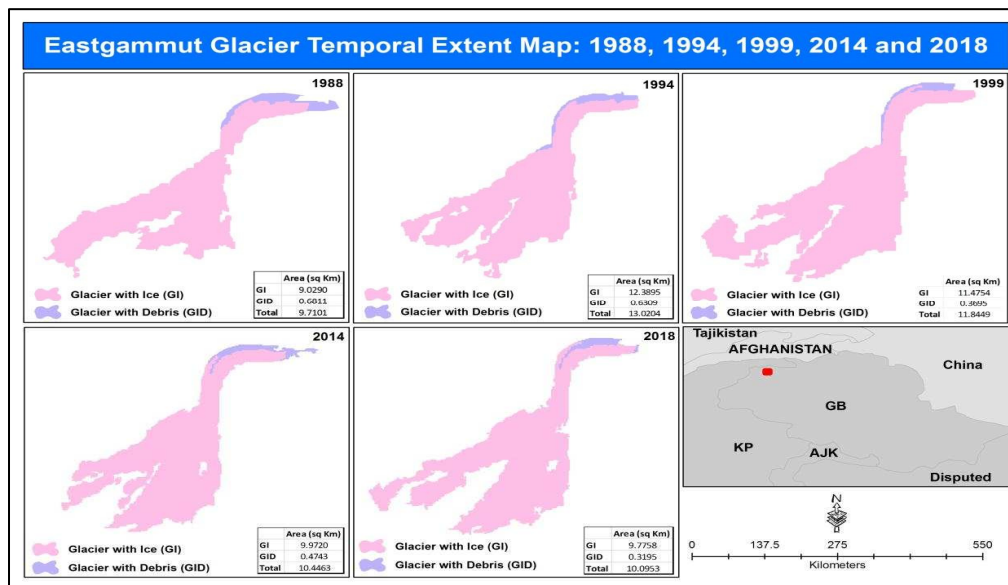

Figure 8. East Gammu glacier temporal change for the years 1988, 1994, 1999, 2014, and 2018.

3.4.4. Karamber Glacier

The extent coordinates of the Karamber glacier are from 74o04' 10'' E to 74o17' 50'' E and from 36o33' 45'' N to 36o40' 22'' N.   Elevation of the glacier goes up to 6,177 m and has a max slope of 74%. Figure 9 shows that the overall ice-covered area from 1988 to 2018 has reduced to 4.74 km². However, the overall debris-covered area from 1988 to 2018 has increased to 2.7 km².
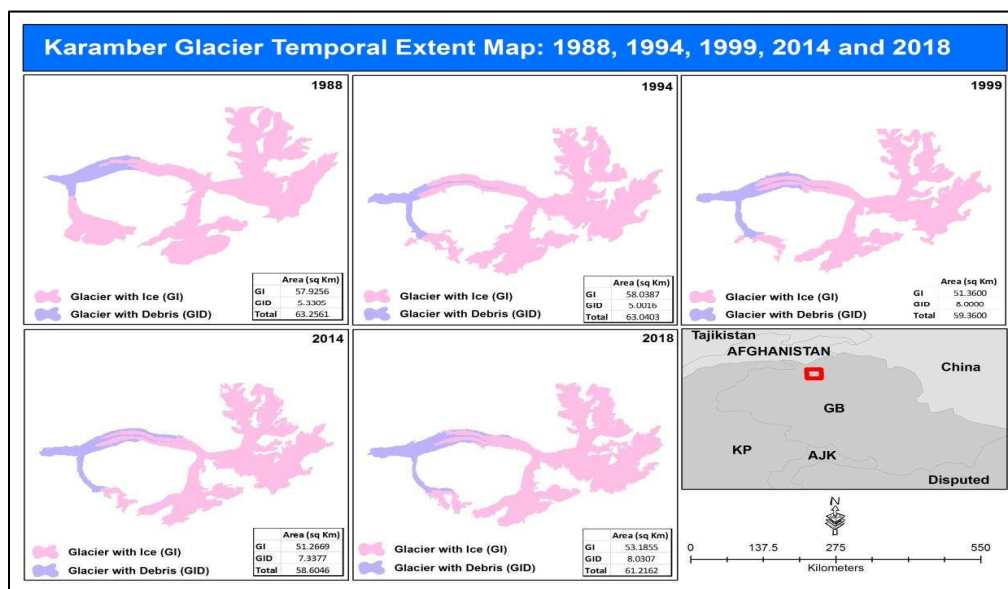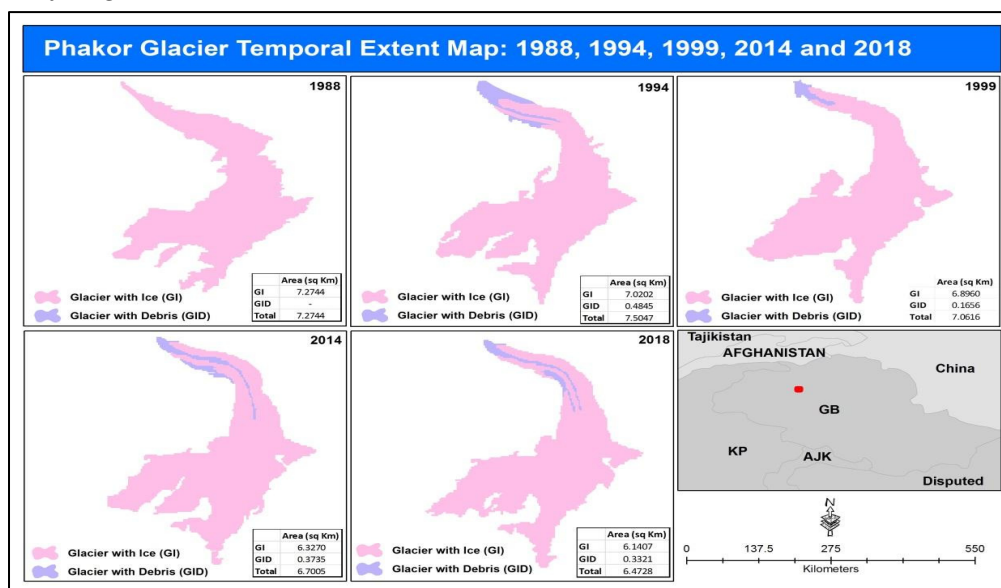

Figure 9. Karamber glacier temporal glacier change extent for 1988, 1994, 1999, 2014, and 2018.

3.4.5. Phakor Glacier

The extent coordinates of the Phakor glacier are from 73o59' 26'' E to 74o02' 03'' E and from 36o18' 02'' N to 36o20' 55'' N. Elevation goes up to 5,531 m and has a max slope of 74%. It was observed that the ice-covered areas are 7.27, 7.02, 6.89, 6.32, and 6.14 km² for the years 1988, 1994, 1999, 2014, and 2018 respectively. Moreover, no debris was found in the year of 1988. The results showed that, the

overall ice-covered area from 1988 to 2018 has decreased to 1.17 sq km. However, the debris-covered area was 0.48, 0.16, 0.37, and 0.33 km^2 for 1994, 1999, 2014, and 2018 respectively. Furthermore, the overall glacier changes are 7.27, 7.50, 7.06, 6.70, and 6.47 km^2 for 1988, 1994, 1999, 2014, and 2018 respectively (Figure 10).

Figure 10. Phakor glacier temporal glacier change extent for 1988, 1994, 1999, 2014, and 2018.

Figure 11 shows the overall summary of the computed glacier areas. Figure 11(a)   shows the aerial extent of the glacier area without debris covering the glacier, i.e., only clear ice glacier has been mapped. The debris cover part of the 5x glaciers has also been mapped, and the total covered area is shown in Figure 11(b). Figure 11(c) shows the sum of clean ice glaciers and debris-covered glaciers to assess the complete extent of the glacier. It is concluded from the graphs that all the galciers remained stable during the last three decades. It shows that precipitation and glacier melts remained almost similar during this period. Similar results were found by [32], when they modeled the water resources and reported the mass balance for the same region. By using the remote sensing, Cao et.al., [33] have also reported that the glaciers of Tibetan Plateau remained stable from 1978 to 2018, despite a misconception that the glaciers are depleting.
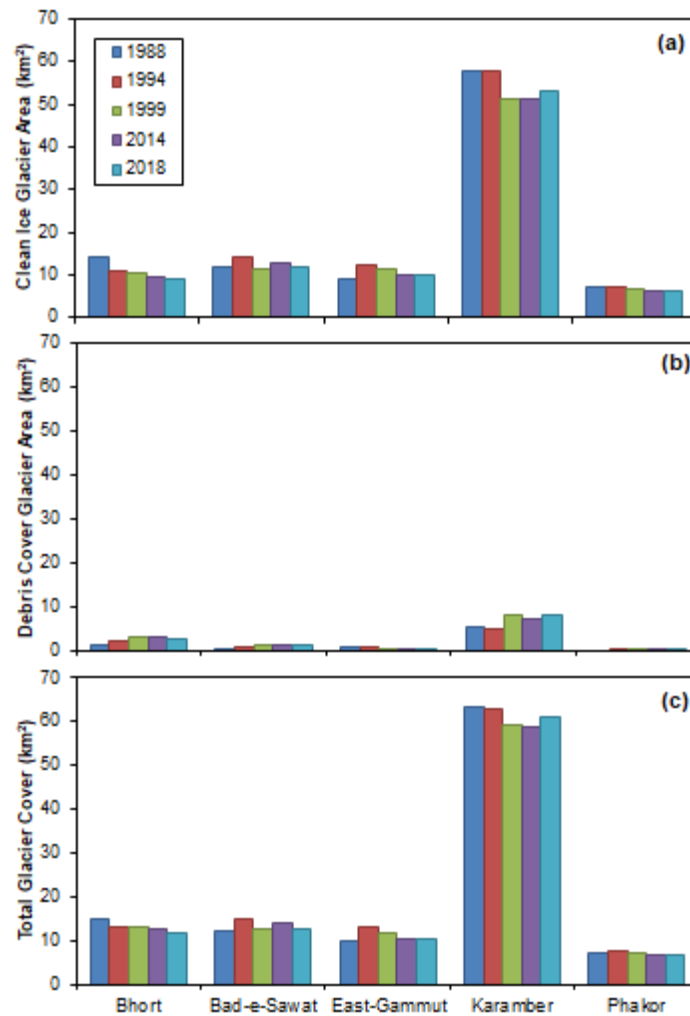
Figure 11. Glacier area changes over the last three decades. (a) clean ice, (b) debris cover, and (c) total basis.

3.5. Accuracy Assessment on Mapping of Glaciers

3.5.1. Error Matrix

Any classification system that comprehends a remotely sensed image will always produce inaccuracy. In order to assess the inaccuracies, the simplest way is the pictorial inspection. We can see mistakes and estimate their size by equating the image with its interpretation results. However, to have a reliable accuracy assessment, it is essential to utilize numerical valuation methods.

A confusion matrix (or error matrix) is a common quantitative tool for determining picture categorization accuracy. A table shows how the categorization result and a reference image correspond. The ground veracity data gathered during the field survey was used to build the error matrix. The results of the ground survey were recorded using a GPS receiver. Table 2 shows the error matrix that was computed. The ground truth classes are in the table's columns, and the classes of the categorised image to be assessed are in the table's rows. The table's cells show the number of pixels for all conceivable correlations between the ground truth and the categorised image.

Table 2. Error matrix.

Class	Glc	Debris	Water bodies	Other (rocks etc.)	Row Total	User Accuracy (UsAc) [on a scale of 0 – 1]
Glacier Cover	133	6	0	3	142	0.937
Debris Cover	8	35	0	0	43	0.814
Water Bodies	0	0	20	1	21	0.952
Other (rocks etc.)	4	0	2	38	44	0.864
Col Total	145	41	22	42	250	
Producer Accuracy (PrAc) [on a scale of 0 – 1]	0.917	0.854	0.909	0.905		

The diagonal essentials of the matrix have been shaded and highlighted. The number of accurately detected pixels is contained in diagonal cells. The entire number of pixels has been divided by the sum of these pixels to give the overall classification accuracy 'p(a),' which equals 87.5 percent. From the equation of Kappa Coefficient, value of Kappa calculated out to be 84.14% which is a good agreement between the ground trothing points and object based classification points.

4. Conclusions

The study investigated glacier cover extent from 1988 to 2018, utilizing remote sensing data for five glaciers (Bhort, Bad-e-Swat, East Gammut, Karamber, and Phakor Glaciers) in the Gilgit River Basin, Karakoram region. Glacier changes were computed based on standard aerial extent measured through object-oriented classification with the help of Landsat satellite imagery.

In the 1961-2000 year period, the averaged monthly series of temperature and other meteorological conditions have been analysised. The min temperature show a temperature range of -36.4 to 22.5 with the highest temperature in July and lowest in February. Apropos, the max solar radiation is in the month of June with a value of 24790 kJ m^{-2} day^{-1} and it's lowest level of 5436 kJ m^{-2} day^{-1} in December. The monthly cumulative precipitation is high in July (111mm) and low in Nov (only at 1mm).

In 1988-2018 period, the Bhort glacier has undergone a loss of glacier surface area from 14.03 sq km to 9.19 sq km whereas Bad-e-Swat glacier, which is also west faced, indicate a small decrease of only ~0.1 sq km, with its area of 11.77 sq km in 1988 to 11.67 sq km in 2018. Bad-e-Swat glacier area show a surging trent in 1994 time when its area was increased to 14.13 sq km. Similarly the East Gammu glacier area seem to have increased from 9 sq km to 12.39 from 1988-1994 and then decreased to 9.9 sq km in 2014. The Karambar glacier, being the largest in the Giglit watershed, remains in 53 sqkm to 58 sq km range in the 30 year time span. Phakor glacier, however, shows a smooth decreasing trend from 1988 till 1999 (~0.04 sqkm every year).

Although, the glaciers in the Gilgit watershed show decreasing trend in the surface area in the 30 year time span, the analysis observes no sign of rapid melting or diminishing of the glaciers. Hence it may be concluded that most of the glaciers in this climate setting remained stable in the Gilgit watershed during the last three decades.

References

1. Stocker, T.F.; Qin, D.; Plattner, G.K.; Tignor, M.M.B.; Allen, S.K.; Boschung, J.; Nauels, A.; Xia, Y.; Bex, V.; Midgley, P.M. *Climate Change 2013: The Physical Science Basis. Contribution of Working Group I to the Fifth Assessment Report of the Intergovernmental Panel on Climate Change*; Cambridge University Press: Cambridge, UK; New York, NY, USA, 2013; pp. 335–344.

2. Barandun, M.; Huss, M.; Usubaliev, R.; Azisov, E.; Berthier, E.; Kääb, A.; Bolch, T.; Hoelzle, M. Multi-decadal mass balance series of three Kyrgyz glaciers inferred from modelling constrained with repeated snow line observations. *Cryosphere* **2018**, *12*, 1899–1919.

3. Ahmad, S.; Israr, M.; Liu, S.; Hayat, H.; Gul, J.; Wajid, S.; Ashraf, M.; Baig, S.U.; Tahir, A.A. Spatio-temporal trends in snow extent and their linkage to hydro-climatological and topographical factors in the Chitral River Basin (Hindukush, Pakistan). *Geocarto International* **2018,** 1-24.

4. Huggel, C.; Kaab, A.; Haeberli, W.; Teysseire, P.; Paul, F. Remote sensing based assessment of hazards from glacier lake outbursts: a case study in the Swiss Alps. *Canadian Geotechnical Journal* **2002**, *39(2)*, 316-330.

5. Immerzeel, W.W.; Van Beek, L.P.H.; Bierkens, M.F.P. Climate change will affect the Asian water towers. *Science* **2010**, *328*, 1382–1385.

6. Muhammad, S.; Tian, L.; Khan, A. Early twenty-first century glacier mass losses in the Indus Basin constrained by density assumptions. *J. Hydrol.* **2019**, *574*, 467–475.

7. Armstrong, R.L.; Rittger, K.; Brodzik, M.J.; Racoviteanu, A.; Barrett, A.P.; Singh Khalsa, S.-J.; Raup, B.; Hill, A.F.; Khan, A.L.; Wilson, A.M.; et al. Runoff from glacier ice and seasonal snow in High Asia: Separating melt water sources in river flow. *Reg. Environ. Chang.* **2019**, *19*, 1249–1261.

8. Zemp, M.; Nussbaumer, S.U.; Gärtner-Roer, I.; Huber, J.; Machguth, H.; Paul, F.; Hoelzle, M. (Eds.) *WGMS (2017) Global Glacier Change Bulletin No. 2 (2014–2015)*; ICSU(WDS)/IUGG(IACS)/UNEP/UNESCO/WMO, *World Glacier Monitoring Service: Zurich, Switzerland*, **1993**, 244.

9. Berthier, E.; Arnaud, Y.; Kumar, R.; Ahmad, S.; Wagnon, P.; Chevallier, P. Remote sensing estimates of glacier mass balances in the himachal pradesh (Western Himalaya, India). *Remote Sens. Environ.* **2007**, *108*, 327–338.

10. Bolch, T.; Kulkarni, A.; Kaab, A.; Huggel, C.; Paul, F.; Cogley, J.G.; Frey, H.; Kargel, J.S.; Fujita, K.; Scheel, M.; Bajracharya, S.; Stoffel, M.. The state and fate of himalayan glaciers. *Science* **2012**, *336*, 310–314.

11. Yao, T.; Thompson, L.; Yang, W.; Yu, W.; Gao, Y.; Guo, X.; Yang, X.; Duan, K.; Zhao, H.; Xu, B.; Pu, J.; Lu.; Ziang, Y.; Kattel, D.B.; Joswiak, D. Different glacier status with atmospheric circulations in Tibetan Plateau and surroundings. *Nature climate change* **2012**, *2(9)*, 663-667.

12. Racoviteanu, A. E.; Armstrong, R.; Williams, M. W. Evaluation of an ice ablation model to estimate the contribution of melting glacier ice to annual discharge in the Nepal Himalaya. *Water Resources Research* **2013**, *49(9)*, 5117-5133.

13. Klare, M. T. Climate Change, Water Scarcity, and the Potential for Interstate Conflict in South Asia. *Journal of Strategic Security* **2020**, *13(4)*, 109-122.

14. Vuille, M.; Francou, B.; Wagnon, P.; Juen, I.; Kaser, G.; Mark, B. G.; Bradley, R. S. Climate change and tropical Andean glaciers: Past, present and future. *Earth-science reviews* **2008**, *89(3-4)*, 79-96.

15. Vuille, M.; Bradley, R. S. Mean annual temperature trends and their vertical structure in the tropical Andes. *Geophysical Research Letters* **2000**, *27(23)*, 3885-3888.

16. Pareta, K.; Pareta, U. New watershed codification system for Indian river basins. *Journal of hydrology and environment research* **2014**, *2(1)*, 31-40.

17. Ali, K.; Bajracharya, R. M.; Sitaula, B. K.; Raut, N.; Koirala, H. L. Morphometric Analysis of Gilgit River Basin in Mountainous Region of Gilgit-Baltistan Province, Northern Pakistan. *Journal of Geoscience and Environment Protection* **2017**, *5(07)*, 70.

18. Zhen, X.; Li, J. Remote Sensing monitoring of glaciers, snow and lake ice in Qinghai-Xizang (Tibetan) Plateau and their Influence on Environments, edited by M. Tang, G. Cheng and Z. Lin *(Guangzhou, China: Guandong Sciences and Technology Press)* **1998** 279-308.

19. Ali, K.; Bajracharya, R. M.; Chapagain, N. R.; Raut, N.; Sitaula, B. K.; Begum, F.; Khan, M.Z; Ali, M.; Ahmed, A. Analyzing Land Cover Change Using Remote Sensing and GIS: A Case Study of Gilgit River Basin, North Pakistan. *International Journal of Economic and Environmental Geology* 2019, *10(1)*, 100-105.

20. Kanwal, S.; Atif, S.; Shafiq, M. GIS based landslide susceptibility mapping of northern areas of Pakistan, a case study of Shigar and Shyok Basins. *Geomatics, Natural Hazards and Risk* **2017** *8(2)*, 348-366.

21. Qaisar, M.; Shafiq, M.; Ghauri, B. M. K.; Younes, I.; Abuzar, M. K. Comparative Analysis of Different Remote Sensing Techniques for Mapping of Supraglacial Lakes on Hispar Glacier. *International Journal of Economic and Environmental Geology* **2019**, *9(2)*, 66-74.

22. Rahim, I.; Ali, S. M.; Aslam, M. GIS Based landslide susceptibility mapping with application of analytical hierarchy process in District Ghizer, Gilgit Baltistan Pakistan. *Journal of Geoscience and Environment Protection* **2018**, *6(2)*, 34-49.

23. Nazeer, A.; Maskey, S.; Skaugen, T.; McClain, M. E. Simulating the hydrological regime of the snow fed and glaciarised Gilgit Basin in the Upper Indus using global precipitation products and a data parsimonious precipitation-runoff model. *Science of the Total Environment* **2022**, *802*, 149872.

24. Willhauck, G.; Schneider, T.; De Kok R.; Ammer U. Comparison of object oriented classification techniques and standard image analysis for the use of change detection between SPOT multispectral satellite images and aerial photos. *Proceedings of XIX ISPRS Congress*, 2000, *33*.

25. Nijhawan, R.;Garg, P.;Thakur, P. A comparison of classification techniques for glacier change detection using multispectral images, *Perspectives in Science* **2016**, *8*, 377-380,

26. Hijmans, R. J., Cameron, S. E., Parra, J. L., Jones, P. G., & Jarvis, A. Very high resolution interpolated climate surfaces for global land areas. *International Journal of Climatology: A Journal of the Royal Meteorological Society* **2005,** *25(15),* 1965-1978.

27. Fick, S.E. and R.J. Hijmans. WorldClim 2: new 1km spatial resolution climate surfaces for global land areas. *International Journal of Climatology* **2017**, *37 (12)*: 4302-4315.

28. Maitima, J.M.; Mugatha, S.M.; Reid, R.S.; Gachimbi, L.N.; Majule, A.; Lyaruu, H.; Pomery, D.; Mathai, S.; Mugisha, S. The linkages between land use change, land degradation and biodiversity across East Africa. *African Journal of Environmental Science and Technology* **2009**, *3(10)*, 310-325.

29. Morgado, P.; Toger, M.; Abrantes, P.; Fiegel, J. A bottom up approach to modeling habitat connectivity dynamics through networks analysis. *Sustainable Development–Authoritative and Leading Edge Content for Environmental Management* **2012**, 131-148.

30. Mukhopadhyay, B.; Khan, A. A reevaluation of the snowmelt and glacial melt in river flows within Upper Indus Basin and its significance in a changing climate. Journal of Hydrology **2015**, 527, 119-132.

31. Javed, ZH., Khan, S., Wahid, A., Ranjha, A. N., Hasan, M., (2020). Climate ofthe Gilgit-Baltistan Province, Pakistan. *International Journal of Economic andEnvironmental Geology*,**2020,** *11(3),* 16-21.

32. Latif, Y.; Ma, Y.; Ma, W.; Muhammad, S.; Adnan, M.; Yaseen, M.; Fealy, R. Differentiating Snow and Glacier Melt Contribution to Runoff in the Gilgit River Basin via Degree-Day Modelling Approach. *Atmosphere* **2020**, *11*, 1023. https://doi.org/10.3390/atmos11101023.

33. Cao, B.; Guan, W.; Li, K.; Wen, Z.; Han, H.; Pan, B. Area and Mass Changes of Glaciers in the West Kunlun Mountains Based on the Analysis of Multi-Temporal Remote Sensing Images and DEMs from 1970 to 2018. *Remote Sens.* **2020**, *12*, 2632. https://doi.org/10.3390/rs12162632.